Ecology, 98(3), 2017, pp. 820–829

Growth rate and resource imbalance interactively control biomass stoichiometry and elemental quotas of aquatic bacteria

Casey M. Godwin [1,2] Emily A. Whitaker,[1,3] and James B. Cotner[1]

[1]*Department of Ecology, Evolution, and Behavior, University of Minnesota, 1987 Upper Buford Circle, Saint Paul, Minnesota 55108 USA*

Abstract. The effects of resource stoichiometry and growth rate on the elemental composition of biomass have been examined in a wide variety of organisms, but the interaction among these effects is often overlooked. To determine how growth rate and resource imbalance affect bacterial carbon (C): nitrogen (N): phosphorus (P) stoichiometry and elemental content, we cultured two strains of aquatic heterotrophic bacteria in chemostats at a range of dilution rates and P supply levels (C:P of 100:1 to 10,000:1). When growing below 50% of their maximum growth rate, P availability and dilution rate had strong interactive effects on biomass C:N:P, elemental quotas, cell size, respiration rate, and growth efficiency. In contrast, at faster growth rates, biomass stoichiometry was strongly homeostatic in both strains (C:N:P of 70:13:1 and 73:14:1) and elemental quotas of C, N, and P were tightly coupled (but not constant). Respiration and cell size increased with both growth rate and P limitation, and P limitation induced C accumulation and excess respiration. These results show that bacterial biomass stoichiometry is relatively constrained when all resources are abundant and growth rates are high, but at low growth rates resource imbalance is relatively more important than growth rate in controlling bacterial biomass composition.

Key words: bacterial biomass composition; carbon; ecological stoichiometry; growth efficiency; homeostasis; phosphorus; relative growth rate; respiration.

Introduction

The interaction between organisms and their resources is a central concept at every level of ecological organization, yet our characterization of these relationships is often oversimplified. Although it is widely understood that resource availability causes changes in the growth rate (Monod 1949) and biomass composition of species (Droop 1974, Bracken et al. 2015), the interdependence of these effects receives little attention. In particular, numerous studies have shown that species differ in how they adjust their biomass stoichiometry in response resource stoichiometry (Sterner and Elser 2002, Persson et al. 2010) or relative growth rate (Elser et al. 2000, Hood et al. 2014), but most studies do not consider the interactive effects of growth rate and resource imbalance. Bacteria are key biogeochemical reactors in all of Earth's ecosystems (Falkowski et al. 2008), so their elemental composition and growth rates determine how they affect the cycles of energy, carbon, and nutrients within ecosystems. Because the stoichiometry of a bacterium's resources is not necessarily the same as the stoichiometry required for biomass and metabolism, bacteria are likely to experience stoichiometric imbalance and low relative growth rates in many ecosystems. Understanding the interactions among resource availability, growth rate, and biomass stoichiometry is key to understanding how biogeochemical cycles will respond to imbalance in the availability of organic carbon and inorganic nutrients (Elser et al. 2009, Peñuelas et al. 2012).

In a seminal paper describing the saturating relationship between resource availability and growth rate, Monod (1949) hypothesized that the biochemical composition of a bacterium is invariant when the cell is growing exponentially near its maximum growth rate (μ_{max}). He reasoned that at μ_{max}, all of the linked processes and reactions necessary for growth operate at some high specific rate, the mean concentrations of all metabolites and cell constituents will be high, and the mean biochemical composition of the cells will converge. One well-studied application of Monod's prediction is the growth rate hypothesis (GRH), which predicts that for P-limited organisms, the demand for P-rich ribosomal RNA at rapid growth rates leads to a positive correlation between growth rate and biomass P content (Elser et al. 2000, Hessen et al. 2013). For heterotrophic bacteria, the growth rate hypothesis is supported by experiments that vary the growth rate of populations and communities in chemostat culture (Chrzanowski and Kyle 1996, Makino et al. 2003, Makino and Cotner 2004). However, comparisons among multiple species of bacteria have found either a weak correlation or no relationship between μ_{max} and P-content (Mouginot et al. 2014,

Manuscript received 20 June 2016; revised 1 October 2016; accepted 29 November 2016. Corresponding Editor: Helmut Hillebrand.

[2]Present address: School of Natural Resources and the Environment, University of Michigan, 440 Church Street, Ann Arbor, Michigan 48109 USA. E-mail: godwi018@umn.edu

[3]Present address: Department of Oceanography, Texas A&M University, 3146 TAMU, College Station, Texas 77843 USA.

Zimmerman et al. 2014, Godwin and Cotner 2015*b*), meaning that the predictive power of the GRH is limited for such comparisons.

Although the original iterations of the GRH were applied to the P-content of biomass, the GRH is frequently extended to predict that biomass C:P and N:P should decline with increasing growth rate. There is support for this extrapolation among phytoplankton, but the effect of $\mu:\mu_{max}$ on biomass stoichiometry is conditionally dependent upon resource imbalance (Goldman et al. 1979, Hillebrand et al. 2013, Garcia et al. 2016). In a recent meta-analysis of multiple phytoplankton species, Hillebrand et al. (2013) showed that phytoplankton biomass N:P was not dependent on growth rate (μ) when N-limited, but N:P decreased with increasing growth rate when P-limited. Some data from phytoplankton (Hillebrand et al. 2013, Garcia et al. 2016) suggest that stoichiometric flexibility could decrease linearly with increasing relative growth rate ($\mu:\mu_{max}$, Fig. 1A, B), but the saturating relationship between internal nutrient quota and growth rate (Droop 1973, Klausmeier et al. 2004) suggests that stoichiometric flexibility should diminish rapidly with increasing $\mu:\mu_{max}$ (Fig. 1C). Alternatively, cells could remain stoichiometrically flexible at higher growth rates by altering their nutrient acquisition rates, cell size (Thingstad et al. 2005), or nutrient use efficiency (Sterner and Elser 2002; Fig. 1D).

It is increasingly acknowledged that heterotrophic bacteria have as much flexibility in $C:P_{biomass}$ and $N:P_{biomass}$ as phytoplankton (Chrzanowski and Kyle 1996, Scott et al. 2012, Godwin and Cotner 2015*a*) and many strains of bacteria increase their C quotas and cell size in response to high resource C:P (Thingstad et al. 2005, Chrzanowski and Grover 2008, Godwin and Cotner 2015*b*). Previous studies that measured stoichiometric flexibility in bacteria did so across a narrow range of relative growth rates (Makino et al. 2003, Scott et al. 2012, Godwin and Cotner 2015*b*) and more comprehensive data are required to determine how flexibility changes with growth rate. Additionally, it is unclear whether the predictions based on phytoplankton N:P would translate to bacterial N:P or C:P. Because C is partitioned between growth and respiration in bacteria, bacterial C:P flexibility could respond to growth rate differently than N:P (in bacteria or phytoplankton). The Droop function can be used to describe the dependence of growth rate on C quota in the same manner as for N or P, but the uptake and accumulation of cellular C are also dependent on growth rate-dependent respiration, growth rate-independent respiration (maintenance metabolism), and energetic costs associated with nutrient limitation (Thingstad 1987). Although respiration could diminish C quotas under some circumstances, its effect on stoichiometric flexibility is uncertain.

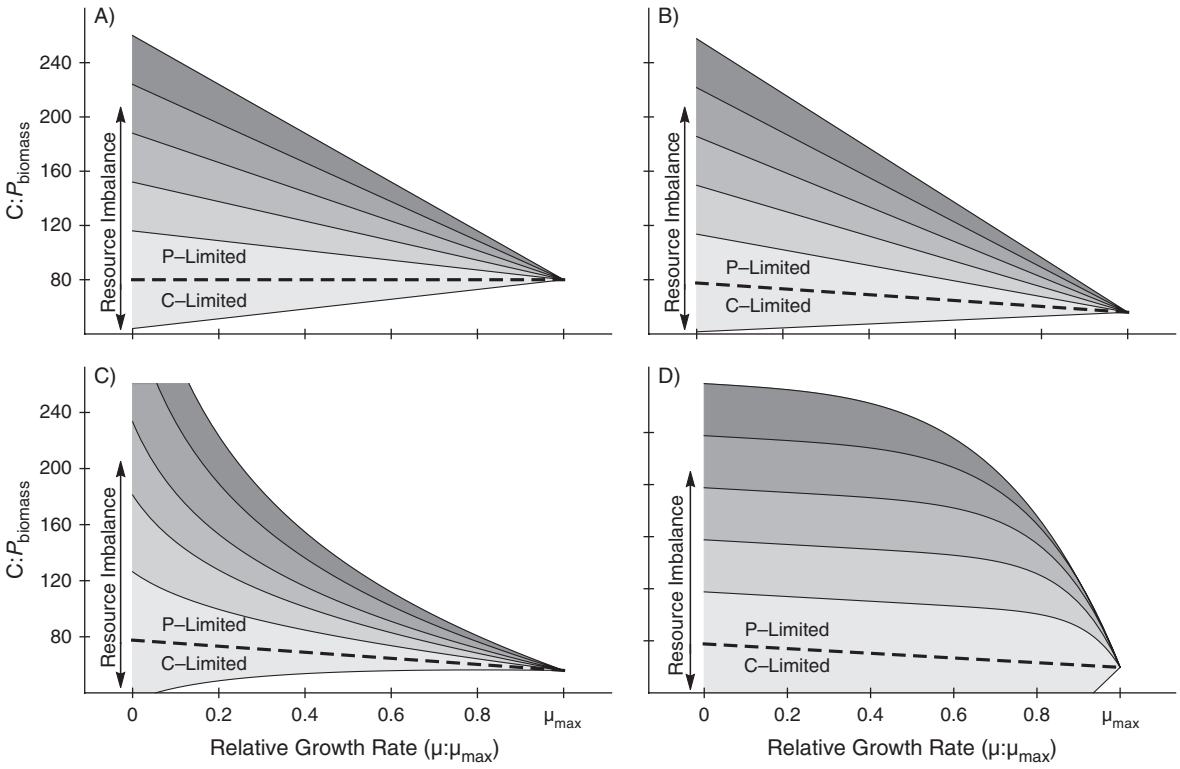

FIG. 1. Schematic plots of $C:P_{biomass}$ versus relative growth rate ($\mu:\mu_{max}$) with different nutrient status scenarios (A–D, after Hillebrand et al. 2013). In all plots, the shading represents varying degrees of nutrient imbalance, as denoted by the arrows. The dashed line represents the biomass stoichiometry under co-limitation and has a negative slope in panels B–D.

Here we describe an experiment where we tested two hypotheses related to the three-way interaction among resource stoichiometry, growth rate, and biomass stoichiometry. Hypothesis 1: For individual strains, stoichiometric flexibility in $C:P_{biomass}$ and $N:P_{biomass}$ decreases nonlinearly with increasing growth rate (Fig. 1C). Hypothesis 2: $C:P_{biomass}$, $N:P_{biomass}$, cell quotas, and cell size increase with resource C:P at low growth rates, but as the growth rate approaches μ_{max}, quotas of C, N, and P increase, cell size increases, and the effect of resource C:P on quotas decreases. To test these hypotheses, we cultured two strains of aquatic heterotrophic bacteria with different growth rates, element quotas, and stoichiometric flexibility in chemostats using a factorial design of varying dilution rate and resource C:P. We describe the interactive effect of growth rate and resource stoichiometry on biomass C:N:P, elemental quotas, cell size, and metabolic rates.

Methods

The two strains of bacteria used for the present study were previously described by Godwin and Cotner (2015*b*). The isolates were selected to provide a contrast in terms of stoichiometric flexibility. *Brevundimonas* strain D703 has highly flexible biomass stoichiometry, a low minimum cell P quota (0.013 fmoles/cell), and an apparent maximum growth rate of 0.159 h^{-1} at 20°C in the defined medium described below. *Achromobacter* strain D1207 has moderately flexible biomass stoichiometry, a higher minimum P quota (0.032 fmoles/cell), and an apparent maximum growth rate of 0.057 h^{-1}. Hereafter, we refer to the strains as *Achromobacter* and *Brevundimonas*. Both strains were preserved as glycerol stocks at −80°C and revived for each culture. Bacteria were grown using basal microbiological medium (BMM, Tanner 2002) with glucose supplied as the sole carbon source at 23.88 mmoles-C/L. Inorganic phosphate in the medium was manipulated to achieve molar $C:P_{supply}$ ratios of 100, 316, 1000, 3162, and 10,000:1. By manipulating the concentration of phosphate in the medium, we were able induce P-limitation at high population densities and cause the bacteria to experience stoichiometric imbalance (Scott et al. 2012, Godwin and Cotner 2014, 2015*a*). For this reason, we denote levels of P supply as $C:P_{supply}$ ratios and also include the P concentration where appropriate. Previous studies using this system have show that bacteria switch from C- to P-limitation at C:P supply ratios between 100 and 300:1 (Scott et al. 2012, Godwin and Cotner 2015*b*). All other inorganic nutrients were supplied in excess relative to the stoichiometric demand for C and P (i.e. C:N = 1.3:1).

Chemostat cultures

Each strain was cultured in duplicate chemostats using a factorial design of $C:P_{supply}$ and dilution rates equivalent to 10, 20, 40, 60, 80, and 95% of their apparent μ_{max} (as measured in nutrient-replete batch cultures). *Brevundimonas* was also cultured at 5% of μ_{max}. Each 100 mL polypropylene chemostat was inoculated with 50 mL of batch culture grown in medium with the same initial $C:P_{supply}$. The chemostats were mixed and aerated with sterile air and maintained at 20°C in darkness. All chemostats were harvested at a single time point. At dilution rates equal to 40% of μ_{max} and greater, the chemostats were harvested after nine times the reciprocal of the dilution rate. To minimize potential wall growth at dilution rates of 20% μ_{max} or less, we monitored the optical density at 600 nm and once the cultures reached steady state biomass, we maintained the cultures for three times the reciprocal of the dilution rate prior to harvesting. Due to low biomass, we obtained limited data from cultures grown using the combination of rapid dilution rate and high $C:P_{supply}$. In total, 133 independent chemostat runs were included in this study. We measured the residual phosphate in the supernatant of centrifuged chemostat cultures using the ascorbic acid molybdenum method (APHA 1995), and used a detection limit equal to the 99% confidence interval for a large number of process blanks.

Biomass elemental analyses

Samples of bacterial biomass were collected onto Whatman GF/F filters (0.7 μm nominal retention) and frozen at −20°C prior to analysis for particulate C, N, and P. Filter samples for C and N determination were dried at 60°C and analyzed using a Perkin Elmer 2400 CHN Analyzer with a zooplankton recovery standard. Filter samples for P determination were digested with acid persulfate and analyzed using the ascorbic acid molybdenum method (APHA 1995) with a spinach leaf recovery standard (NIST reference material). Process filter blanks were included in each run and were used to determine detection limits (99% confidence level). We have shown previously that small amounts of non-bacterial C and N from the medium are retained on the filters (<1% of the C and N measured on filters in this study), but there was no significant retention of P (Godwin and Cotner 2015*a*).

Flow cytometry

Cells of *Achromobacter* formed small aggregates that could not be completely dispersed and therefore flow cytometry data are not presented for this strain. Samples from *Brevundimonas* were preserved with buffered formaldehyde to a final concentration of 3.7% and stored at 4°C until use. Duplicate samples from each culture were diluted with sodium pyrophosphate and vortexed to improve cell dispersion (Velji and Albright 1993). Fluorescent beads (Spherotech) were added to each sample as an internal standard to enumerate cells. Bead stocks were assayed daily by epifluorescence microscopy. Samples were stained with SybrGreen (Invitrogen, Carlsbad, California, USA)

to a final concentration of 0.05% and incubated for at least 10 minutes prior to analysis. Cytometry was performed using a Becton Dickson FACSCalibur with a 488 nm laser. Side scatter and fluorescence at 530 nm were used to identify populations of cells and beads. At least 9,000 cell events were recorded for each sample.

Respirometry

To measure the rate of O_2 consumption and CO_2 production, we incubated air-equilibrated samples from the chemostats in 6 mL gas-tight vials at 22°C. At multiple time points up to 2 h, we preserved the samples with mercuric chloride to a final concentration of 0.015% and stored the vials at 4°C until analysis by membrane-inlet mass spectrometry (Kana 1994). The oxygen concentration was determined using the O_2:Ar method (Kana 1994) with air-equilibrated BMM medium as a reference standard. Carbon dioxide content was determined using a cryotrap at −140°C, which retained water vapor but allowed CO_2 to be measured. Flasks of BMM with mercuric chloride were saturated with calibrated gas standards of CO_2 and used to determine the pCO_2 in each sample. The total CO_2 in each sample was determined from pCO_2 and the estimated endpoint pH after the addition of mercuric chloride and pCO_2 from respiration. Respiration rates were calculated as the decrease in O_2 or increase in total CO_2 per unit time and normalized to cell abundance for *Brevundimonas*. The rate of biomass production at steady state was calculated as the product of the C quota and the dilution rate. The apparent bacterial growth efficiency was calculated as the ratio of biomass production to the sum of production and respiration.

Batch cultures

We performed a parallel experiment to the chemostats, but using batch cultures grown in the same medium. The objectives of this experiment were to (1) characterize biomass stoichiometry at μ_{max} (which is difficult in chemostats) and determine whether batch cultures could be used to provide a similar measurement of stoichiometric flexibility as the chemostats. The initial concentration of C and P would not be limiting in batch cultures, even at high C:P. But as population growth depletes the resources, C or P becomes limiting and the growth rate decreases in response. We sought to measure the biomass stoichiometry during the initial density-independent phase and at multiple points during density dependence. At each level of $C:P_{supply}$ used for the chemostats, we inoculated 24 cultures (100 mL) with varying volumes of frozen glycerol stocks and incubated the cultures at 22–24°C on an orbital shaker. Because multiple simultaneous cultures were used for this experiment, we consolidated these growth curves using simple models based on population densities (optical density at 600 nm, OD_{600}). For each individual batch culture, consecutive OD_{600} measurement pairs were used to compute instantaneous growth rates. Population growth was modeled as density-dependent for $C:P_{supply}$ of 3,162:1 and 10,000:1 and using a biphasic model with density-independent growth followed by density dependence for $C:P_{supply}$ of 100:1 to 1,000:1 (Appendix S1).

Statistical analyses

For the chemostat culture experiment, a two-way analysis of variance (ANOVA) was used for each strain to examine the effects of growth rate, log $C:P_{supply}$, and their interaction on the dependent variables. Biomass stoichiometric ratios were log-transformed prior to ANOVA to improve normality. We were unable to test for an interaction between growth rate and medium C:P in the batch cultures because the range of population density and growth rate attained was different for each C:P treatment. In batch culture samples where the bacteria were growing at μ:μmax of 95% or more, we evaluated the effect of $C:P_{supply}$ by one-way ANOVA. All statistical analyses were performed using R version 3.2.3 (R Core Team 2015).

Results

Chemostats

Biomass yields decreased with increasing $C:P_{supply}$ (i.e., decreasing P concentration) in both strains, but at low $\mu:\mu_{max}$ the biomass of *Brevundimonas* was highest at $C:P_{supply}$ of 316:1 (Appendix S1: Fig. S2). At $C:P_{supply}$ of 316:1 and greater, both strains depleted the available phosphate to low levels, depending upon $\mu:\mu_{max}$ (Appendix S1: Figs. S3 and S4). Biomass stoichiometry for *Brevundimonas* ranged from C:N:P of 47:9:1 to 618:86:1 and in *Achromobacter* it ranged from 42:8:1 to 290:35:1 (Fig. 2). All three elemental ratios ($C:P_{biomass}$, $N:P_{biomass}$, and $C:N_{biomass}$) were strongly affected by $C:P_{supply}$ in both strains (Fig. 2; Appendix S1: Figs. S5 and S6). Growth rate and the interaction between growth rate and $C:P_{supply}$ also had strong effects on the biomass stoichiometry of each strain, but in *Achromobacter* the interaction was significant for $C:P_{biomass}$ and $N:P_{biomass}$ only ($P < 0.05$). In both strains, $C:P_{supply}$ had no significant effect on biomass stoichiometry at high $\mu:\mu_{max}$. At a $C:P_{supply}$ of 100:1, biomass ratios in *Achromobacter* were not significantly affected by growth rate, but for *Brevundimonas*, $C:P_{biomass}$ and $C:N_{biomass}$ ratios decreased in response to increasing $\mu:\mu_{max}$ (Fig. 2; Appendix S1: Figs. S5 and S6).

In *Brevundimonas*, both P and C quotas were strongly affected by $C:P_{supply}$ and growth rate, but only the P quota showed a significant interaction between $C:P_{supply}$ and growth rate (Fig. 2). At low $\mu:\mu_{max}$, P quotas decreased markedly between $C:P_{supply}$ of 100:1 and 316:1. At $\mu:\mu_{max}$ of 60% or greater, the P-quotas were substantially higher and increased with increasing $C:P_{supply}$. At every $\mu:\mu_{max}$, C quotas increased with increasing $C:P_{supply}$ and the C quota was generally higher at high growth rates. When analyzed across levels of $C:P_{supply}$, the correlation coefficient between C and P quotas was negative at

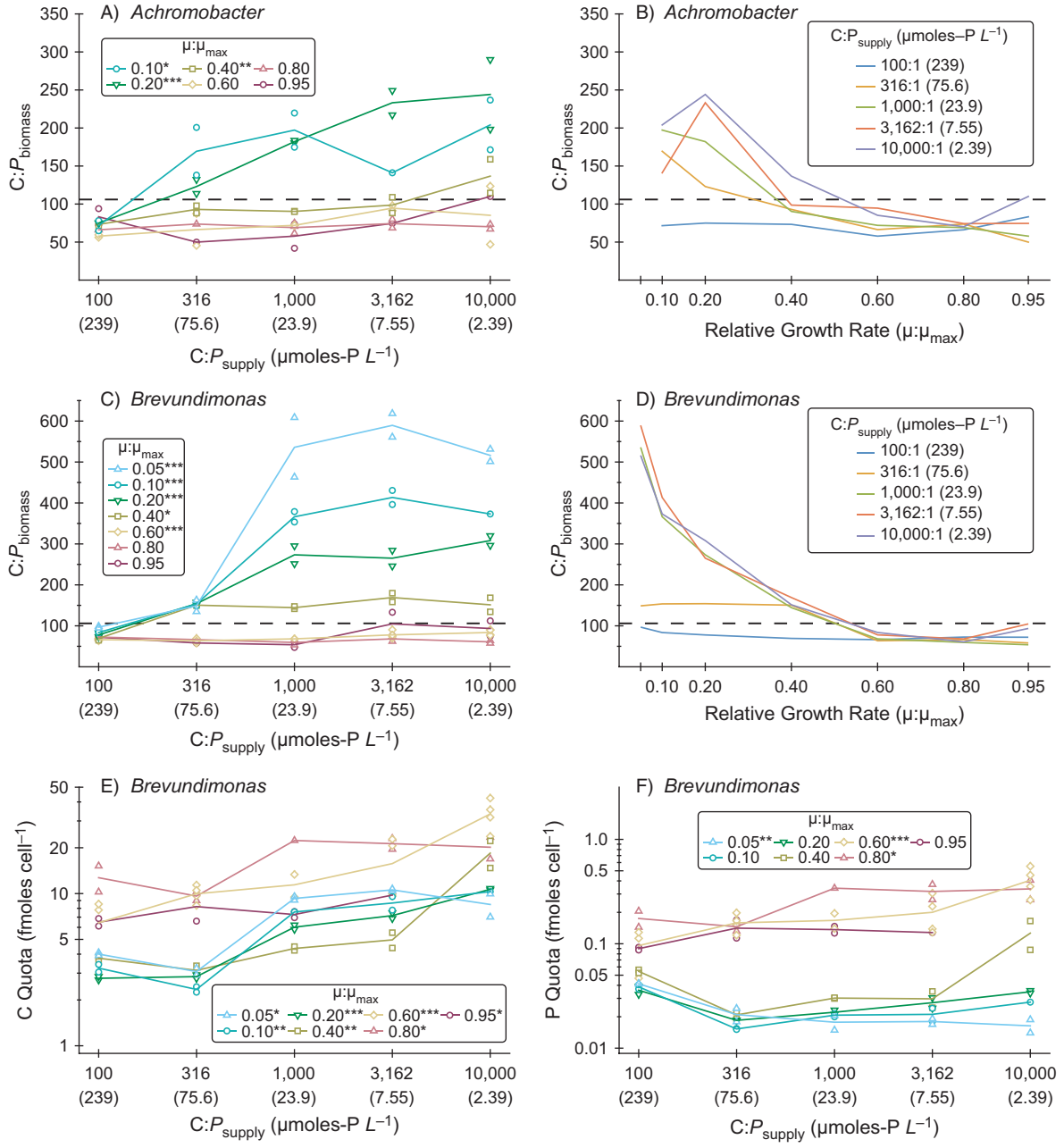

FIG. 2. Biomass C:P as a function of $C:P_{supply}$ and relative growth rate ($\mu:\mu_{max}$) for *Achromobacter* (A, B) and *Brevundimonas* (C, D). Lines are segmented fits to the mean values and the points are the replicate chemostat and the black dashed lines represent the Redfield ratio of $C:P_{biomass}$ = 106:1. For each strain, the two-way ANOVA tests showed significant effects of $C:P_{supply}$, $\mu:\mu_{max}$, and an interaction (all $P < 0.01$) for $C:P_{biomass}$. Cell quotas of C and P for *Brevundimonas* across $C:P_{supply}$ (E, F). The two-way ANOVA tests showed significant effects of $C:P_{supply}$, $\mu:\mu_{max}$, and an interaction (all $P < 0.01$) for P quotas and significant effects of $C:P_{supply}$ and $\mu:\mu_{max}$ for C quotas ($P < 0.001$). The significance of one-way ANOVA tests at each level of $\mu:\mu_{max}$ is denoted in the legends (*$P < 0.05$, **$P < 0.01$, ***$P < 0.001$). [Color figure can be viewed at wileyonlinelibrary.com]

5% μ_{max}, then increased to a strong positive correlation between 40% and 80% of μ_{max}, and declined again at 95% μ_{max}. Quotas of C and N were strongly correlated at every level of $\mu:\mu_{max}$ ($r^2 > 0.95$).

The flow cytometry characteristics of *Brevundimonas* were responsive to both $C:P_{supply}$ and growth rate (Appendix S1: Fig. S7). These changes in flow cytometry observations were consistent with cell elongation in response to P limitation, as observed in a previous study with these strains (Godwin and Cotner 2015*b*). At $\mu:\mu_{max}$ of 5–40%, SybrGreen fluorescence (proportional to DNA content), side scatter, and forward scatter all increased

with increasing C:P_{supply}. At $\mu:\mu_{max}$ of 60–95%, the flow cytometry characteristics were much less sensitive to C:P_{supply}. At C:P_{supply} of 100 to 316:1, the cells became larger at faster growth rates. But at higher C:P_{supply}, the cells became smaller at faster growth rates. At 5 to 20% $\mu:\mu_{max}$, both cell size and C quota increased in response to increasing C:P_{supply} (Appendix S1: Figs. S9 and S10). At 60% $\mu:\mu_{max}$, the cells remained the same size and the quotas of C, N, and P increased in response to increasing C:P_{supply}.

For *Brevundimonas*, both O_2 consumption and CO_2 production showed strong effects of C:P_{supply}, growth rate, and an interaction. At low growth rates, cell-specific respiration rates (both O_2 and CO_2) increased with increasing C:P_{supply}. At higher growth rates, the respiration rates were much higher and were less sensitive to C:P_{supply}. The apparent bacterial growth efficiency (BGE) ranged from about 30–80% (Fig. 3) and was most sensitive to C:P_{supply} at low $\mu:\mu_{max}$, decreasing from 60% at C:P_{supply} of 100:1 to less than 40% at C:P_{supply} greater than 1,000:1.

Batch cultures

In batch cultures, both strains exhibited variable growth rates in response to population density and phosphorus availability (Appendix S1: Fig. S1, Table S1). At high C:P_{supply} neither strain was observed to grow at its apparent μ_{max}. In early batch culture, when the growth rate was density-independent (at or near μ_{max}), the bacterial biomass stoichiometry was not sensitive to resource stoichiometry. During density-dependent growth, the biomass stoichiometry was sensitive to both the resource stoichiometry and the growth rate. For both strains, the chemostats and batch cultures showed that C:$P_{biomass}$ decreased with growth rate and the that effect was most profound at high C:P_{supply} (Fig. 4). In batch cultures at C:P_{supply} of 100:1, the C:$P_{biomass}$ stoichiometry increased slightly with growth rate in *Brevundimonas* ($P < 0.01$) and was not correlated with growth rate in *Achromobacter*. At every level of C:P_{supply}, decreasing growth rate in the batch cultures led to a significant reduction in the P quota of *Brevundimonas*. Carbon quotas also decreased at lower growth rates although this was only significant for C:P_{supply} of 100 to 3162:1.

Biomass stoichiometry (C:P, N:P, and C:N) did not differ between quickly-growing chemostat cultures (80–95% $\mu:\mu_{max}$) and batch cultures where the instantaneous growth rate was >95% of μ_{max} (*t*-test $P > 0.05$). At high growth rate, the median C:N:$P_{biomass}$ was 73:14:1 for *Brevundimonas* (95% confidence interval: C:$P_{biomass}$ of 68.5–77.4 and N:$P_{biomass}$ of 12.8–14.2:1) and 70:13:1 for *Achromobacter* (95% CI: C:$P_{biomass}$ of 62.6–76.7 and N:$P_{biomass}$ of 11.8–13.7).

Discussion

Here we show that relative growth rate strongly modified the relationship between resource stoichiometry and bacterial biomass composition. Overall, the physiology of the bacteria and their response to P availability was markedly different at low versus high $\mu:\mu_{max}$, with the most extreme biomass stoichiometry observed at the lowest growth rates. In the following sections, we discuss the effect of this interaction on biomass stoichiometry, element quotas, size, and respiration.

We hypothesized that for individual strains, stoichiometric flexibility decreases nonlinearly with increasing $\mu:\mu_{max}$. This hypothesis was supported in both strains and the biomass stoichiometry was essentially homeostatic at $\mu:\mu_{max}$ greater than 50%. The nonlinear pattern in Fig. 2 (panels B and D) resembles the pattern depicted in Fig. 1C and is consistent with the limited data for heterotrophic bacteria (Makino and Cotner 2004) and previous studies in phytoplankton (Goldman et al. 1979, Hillebrand et al. 2013). A recent chemostat study with the cyanobacterium

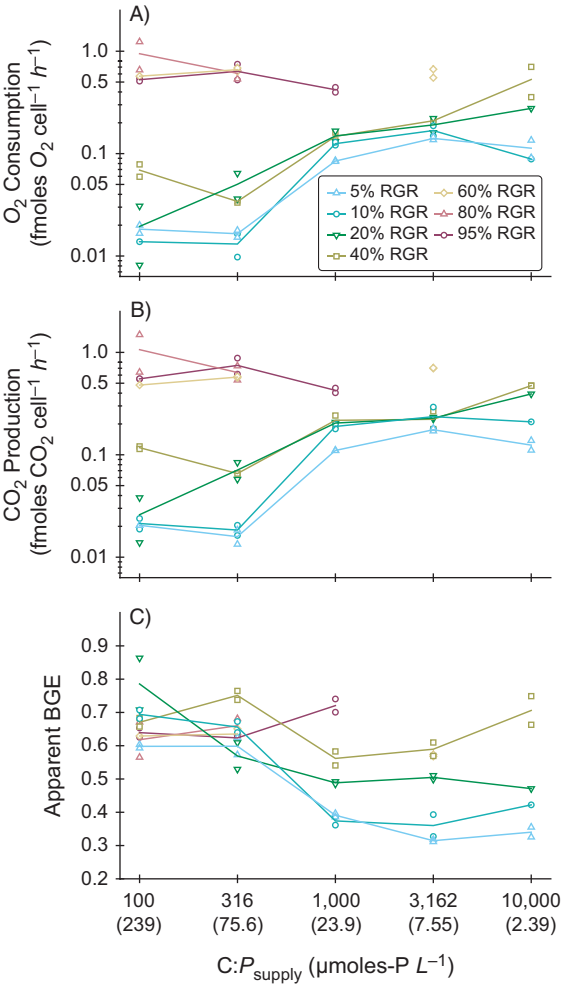

FIG. 3. Cell-specific O_2 consumption rate (A), CO_2 production rate (B), and bacterial growth efficiency (C) for *Brevundimonas* as a function of C:P_{supply}, with separate symbols for levels of $\mu:\mu_{max}$. The two-way ANOVA tests showed significant effects of C:P_{supply}, $\mu:\mu_{max}$, and an interaction for O_2 consumption, CO_2 production, and BGE ($P < 0.01$). [Color figure can be viewed at wileyonlinelibrary.com]

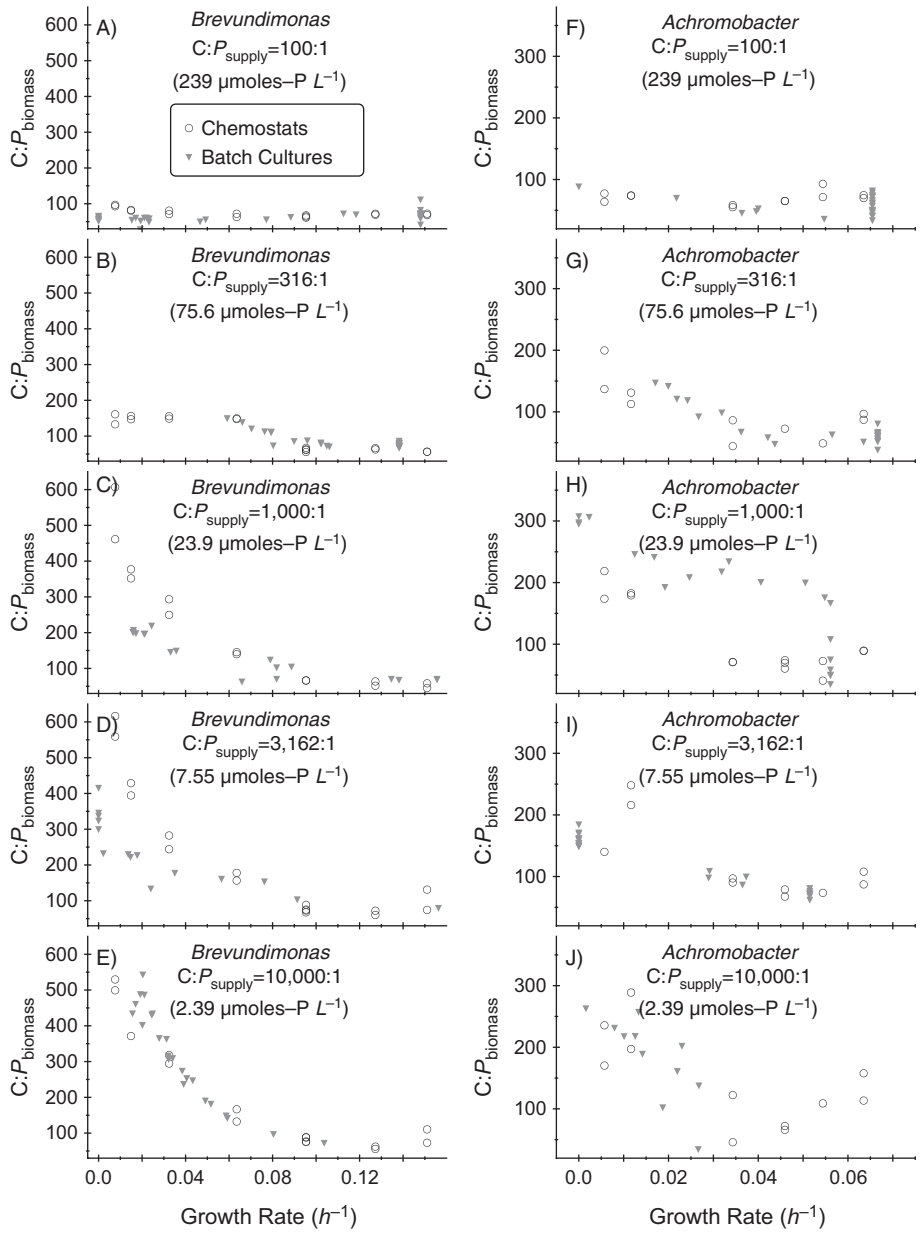

FIG. 4. Dependence of bacterial $C:P_{biomass}$ on growth rate (μ, h^{-1}) at each level of $C:P_{supply}$. Panels A–J contain data from both chemostats and batch cultures. Growth rates for batch cultures are predicted from the growth models described in Appendix S1.

Synechococcus found that under P limitation, $N:P_{biomass}$ decreased linearly with growth rate between $\mu:\mu_{max}$ of 0 to about 70% (Garcia et al. 2016). Across a similar range of $\mu:\mu_{max}$, our data for $C:P_{biomass}$ and $N:P_{biomass}$ are distinctly nonlinear (Fig. 2; Appendix S1: Fig. S5), which suggests that surplus accumulation of C and N was more pronounced in this heterotrophic bacterium.

The nonlinear response of $C:P_{biomass}$ and $N:P_{biomass}$ to increasing $\mu:\mu_{max}$ is attributable to the saturating relationship between internal quotas and growth rate, as described by the Droop cell quota model (Droop 1974, Thingstad 1987, Klausmeier et al. 2004). At low $\mu:\mu_{max}$, the quota of any element that limits the growth rate approaches its minimum quota, so the quota of non-limiting elements can vary substantially in response to surplus availability (Chrzanowski and Kyle 1996, Vrede et al. 2002, Thingstad et al. 2005, Godwin and Cotner 2015*b*). At higher $\mu:\mu_{max}$, the quotas of all elements approach their values at μ_{max} and the quota of any single element becomes less flexible than at low $\mu:\mu_{max}$. As a result, the stoichiometric ratio of any two elements becomes less flexible at high $\mu:\mu_{max}$. The effective μ_{max} can be different for each element in the Droop model (Cherif and Loreau 2010, Garcia et al. 2016), which

contributes to the nonlinear pattern in biomass stoichiometry at increasing growth rates. Although we were unable to parameterize the Droop model for C and N in our experiment, our estimates of effective μ_{max} based on P quotas under P limitation ($C:P_{supply}$ >100:1) were substantially lower than the actual μ_{max} for *Brevundimonas* (Appendix S1: Fig. S8).

It is clear that elemental ratios can overlook important trends in quotas. We hypothesized that $C:P_{biomass}$, $N:P_{biomass}$, cell quotas, and cell size would increase with resource C:P at low growth rates, but as the growth rate approaches μ_{max}, quotas of C, N, and P would increase, cell size would increase, and the effect of resource C:P on quotas would decrease. Overall, the chemostat experiments support our hypotheses, but there were important deviations from our expectations. At low growth rates, P quotas were negatively coupled to C and N quotas in *Brevundimonas* and plasticity in C and N quotas was associated with an increase in cell size under P-limitation, which has been described previously for this isolate and other aquatic bacteria (Thingstad et al. 2005, Godwin and Cotner 2015*b*). In contrast, at high $\mu:\mu_{max}$, element ratios and cell size were constrained, which seems to suggest homeostatic composition. However, the C, N, and P quotas at high $\mu:\mu_{max}$ varied substantially in response to growth rate and $C:P_{supply}$ (Fig. 2; Appendix S1: Figs. S9 and S10). This finding indicates strong positive coupling of C, N, and P quotas at high growth rates, which is predicted by the Droop model (Droop 1973).

There were strong effects of both growth rate and P availability on the relationship between cell size and C quota. Cell size is expected to increase with increasing growth rate (Vadia and Levin 2015, Garcia et al. 2016). Cell size increased somewhat with growth rate at $C:P_{supply}$ of 100:1 and 316:1, but the cells became smaller with increasing growth rate at higher $C:P_{supply}$. High $C:P_{supply}$ ratios tend increase bacterial cell volume and C quotas (Thingstad et al. 2005, Godwin and Cotner 2015*b*), but in *Brevundimonas* this effect was only apparent at low $\mu:\mu_{max}$ (Appendix S1: Fig. S9). At higher $\mu:\mu_{max}$, the cells changed their C quota substantially but cell size changed very little. Although we expected C and N quotas to increase at high $\mu:\mu_{max}$, the quotas were highest at $\mu:\mu_{max}$ of 60% (Fig. 2; Appendix S1: Fig. S8). Combined with the observation that cell size changed little above 60% $\mu:\mu_{max}$, it is apparent that the cells changed their C content independently of size. This behavior is dramatically different from the plasticity observed at low $\mu:\mu_{max}$ and the behavior of *Synechococcus* (Garcia et al. 2016). Importantly, the strong correlation between C and N quotas suggests that this surplus accumulation was not due to C-rich storage polymers (Sterner and Elser 2002).

The respiration rate of *Brevundimonas* increased with $\mu:\mu_{max}$, consistent with models of bacterial metabolism (Thingstad 1987, Russell and Cook 1995), but there was also a dramatic effect of $C:P_{supply}$ on respiration rate. At all $\mu:\mu_{max}$ below 50%, increasing $C:P_{supply}$ (decreasing P availability) led to a several-fold increase in the respiration rate and a decrease in bacterial growth efficiency. The increase in specific respiration rate at high $C:P_{supply}$ is similar to the respiration of excess C by phagotrophs consuming C-rich but nutrient-poor prey items (Frost et al. 2005, Jeyasingh 2007, Hessen and Anderson 2008). However, osmotrophic heterotrophs should not need to consume excess C at high resource C:P in order to obtain inorganic P. One explanation for this response is that under these conditions, the uptake and respiration of glucose were decoupled from the immediate growth demands of the bacteria (Russell and Cook 1995). A possible reason for this decoupling is that high-affinity P-uptake mechanisms increased the energetic demands of the bacterium (Rosenberg et al. 1979), leading to an increase in respiration rate relative to the growth rate-dependent rate (Tempest and Neijssel 1978, Thingstad 1987). These mechanisms are heavily dependent upon intracellular ATP and phosphate, which would seem a contradictory strategy under P-limitation, unless ATP turnover is rapid (Russell and Cook 1995).

Experiments to characterize stoichiometric physiology have important design limitations. The present study shows that data from batch cultures and chemostats are comparable when growth rates approach μ_{max}, but during density-dependent growth the two methods showed inconsistent agreement. Although batch cultures might yield the same physiological state as steady-state chemostat cultures, the transient nature of both resource concentration and growth rate in batch cultures makes it difficult to separate the effect of resource availability from that of growth rate. This methodological issue is important for characterizing the stoichiometric physiology of other osmotrophic organisms such as phytoplankton. Meta-analyses that combine data from batch cultures and continuous cultures require careful interpretation (Persson et al. 2010), but can also identify broad-scale patterns that are difficult to detect in individual studies (Hillebrand et al. 2013). Ongoing efforts to characterize stoichiometric flexibility in diverse taxa would benefit from robust high-throughput methods for measuring biomass composition.

Our study shows that resource imbalance controls bacterial biomass stoichiometry and element quotas at low growth rates, but when growth rate exceeds about 50% of μ_{max}, resource imbalance has little impact on biomass stoichiometry and C, N, and P quotas increase proportionally in response to resource imbalance and growth rate. Based on this work and previous studies, bacterial biomass can be modeled as a flexible pool of C, N, and P at low growth rates. It is increasingly recognized that stoichiometric flexibility has important implications for biogeochemical cycles (Galbraith and Martiny 2015). Although the majority of bacterial isolates from lakes exhibit stoichiometric flexibility at low $\mu:\mu_{max}$ (Scott et al. 2012, Godwin and Cotner 2014), mass balance models typically assume a fixed stoichiometry for their biomass. However, for bacteria growing at high $\mu:\mu_{max}$, our results support the use of models with homeostatic biomass stoichiometry.

Acknowledgments

This manuscript was improved following comments from three anonymous reviewers. This work was supported by NSF-IOS award 1257571 to JBC.

Literature Cited

APHA. 1995. Standard methods for the examination of water and wastewater: including bottom sediments and sludges. Twentieth edition. American Public Health Association, New York, New York, USA.

Bracken, M. E. S., et al. 2015. Signatures of nutrient limitation and co-limitation: responses of autotroph internal nutrient concentrations to nitrogen and phosphorus additions. Oikos 124:113–121.

Cherif, M., and M. Loreau. 2010. Towards a more biologically realistic use of Droop's equations to model growth under multiple nutrient limitation. Oikos 119:897–907.

Chrzanowski, T. H., and J. P. Grover. 2008. Element content of *Pseudomonas fluorescens* varies with growth rate and temperature: A replicated chemostat study addressing ecological stoichiometry. Limnology and Oceanography 53:1242–1251.

Chrzanowski, T. H., and M. Kyle. 1996. Ratios of carbon, nitrogen and phosphorus in *Pseudomonas fluorescens* as a model for bacterial element ratios and nutrient regeneration. Aquatic Microbial Ecology 10:115–122.

Droop, M. R. 1973. Some thoughts on nutrient limitation in algae. Journal of Phycology 9:264–272.

Droop, M. R. 1974. The nutrient status of algal cells in continuous culture. Journal of the Marine Biological Association of the United Kingdom 54:825–855.

Elser, J. J., R. W. Sterner, E. Gorokhova, W. F. Fagan, T. A. Markow, J. B. Cotner, J. F. Harrison, S. E. Hobbie, G. M. Odell, and L. J. Weider. 2000. Biological stoichiometry from genes to ecosystems. Ecology Letters 3:540–550.

Elser, J. J., T. Andersen, J. S. Baron, A.-K. Bergström, M. Jansson, M. Kyle, K. R. Nydick, L. Steger, and D. O. Hessen. 2009. Shifts in lake N: P stoichiometry and nutrient limitation driven by atmospheric nitrogen deposition. Science 326:835–837.

Falkowski, P. G., T. Fenchel, and E. F. Delong. 2008. The microbial engines that drive Earth's biogeochemical cycles. Science 320:1034–1039.

Frost, P. C., M. A. Evans-White, Z. V. Finkel, T. C. Jensen, and V. Matzek. 2005. Are you what you eat? Physiological constraints on organismal stoichiometry in an elementally imbalanced world. Oikos 109:18–28.

Galbraith, E. D., and A. C. Martiny. 2015. A simple nutrient-dependence mechanism for predicting the stoichiometry of marine ecosystems. Proceedings of the National Academy of Sciences USA 112:8199–8204.

Garcia, N. S., J. A. Bonachela, and A. C. Martiny. 2016. Interactions between growth-dependent changes in cell size, nutrient supply and cellular elemental stoichiometry of marine Synechococcus. ISME Journal. https://doi.org/10.1038/ismej.2016.50

Godwin, C. M., and J. B. Cotner. 2014. Carbon:phosphorus homeostasis of aquatic bacterial assemblages is mediated by shifts in assemblage composition. Aquatic Microbial Ecology 73:245–258.

Godwin, C. M., and J. B. Cotner. 2015*a*. Aquatic heterotrophic bacteria have highly flexible phosphorus content and biomass stoichiometry. ISME Journal. https://doi.org/10.1038/ismej.2015.34

Godwin, C. M., and J. B. Cotner. 2015*b*. Stoichiometric flexibility in diverse aquatic heterotrophic bacteria is coupled to differences in cellular phosphorus quotas. Frontiers in Microbiology 6. https://doi.org/10.3389/fmicb.2015.00159

Goldman, J. C., J. J. McCarthy, and D. G. Peavey. 1979. Growth-rate influence on the chemical composition of phytoplankton in oceanic waters. Nature 279:210–215.

Hessen, D. O., and T. R. Anderson. 2008. Excess carbon in aquatic organisms and ecosystems: physiological, ecological, and evolutionary implications. Limnology and Oceanography 53:1685–1696.

Hessen, D. O., J. J. Elser, R. W. Sterner, and J. Urabe. 2013. Ecological stoichiometry: an elementary approach using basic principles. Limnology and Oceanography 58:2219–2236.

Hillebrand, H., G. Steinert, M. Boersma, A. Malzahn, C. Léo Meunier, C. Plum, and R. Ptacnik. 2013. Goldman revisited: faster growing phytoplankton has lower N: P and lower stoichiometric flexibility. Limnology and Oceanography 58:2076–2088.

Hood, J. M., R. W. Sterner, and M. Pfrender. 2014. Carbon and phosphorus linkages in *Daphnia* growth are determined by growth rate, not species or diet. Functional Ecology 28:1156–1165.

Jeyasingh, P. D. 2007. Plasticity in metabolic allometry: the role of dietary stoichiometry. Ecology Letters 10:282–289.

Kana, T. M. 1994. Membrane inlet mass spectrometer for rapid high-precision determination of N_2, O_2, and Ar in environmental water samples. Analytical Chemistry 66: 4166–4170.

Klausmeier, C. A., E. Litchman, and S. A. Levin. 2004. Phytoplankton growth and stoichiometry under multiple nutrient limitation. Limnology and Oceanography 49: 1463–1470.

Makino, W., and J. B. Cotner. 2004. Elemental stoichiometry of a heterotrophic bacterial community in a freshwater lake: implications for growth- and resource-dependent variations. Aquatic Microbial Ecology 34:33–41.

Makino, W., J. B. Cotner, R. W. Sterner, and J. J. Elser. 2003. Are bacteria more like plants or animals? Growth rate and resource dependence of bacterial C: N: P stoichiometry. Functional Ecology 17:121–130.

Monod, J. 1949. The growth of bacterial cultures. Annual Reviews in Microbiology 3:371–394.

Mouginot, C., R. Kawamura, K. L. Matulich, R. Berlemont, S. D. Allison, A. S. Amend, and A. C. Martiny. 2014. Elemental stoichiometry of fungi and bacteria strains from grassland leaf litter. Soil Biology and Biochemistry 76:278–285.

Peñuelas, J., J. Sardans, A. Rivas-ubach, and I. A. Janssens. 2012. The human-induced imbalance between C, N and P in Earth's life system. Global Change Biology 18:3–6.

Persson, J., P. Fink, A. Goto, J. M. Hood, J. Jonas, and S. Kato. 2010. To be or not to be what you eat: regulation of stoichiometric homeostasis among autotrophs and heterotrophs. Oikos 119:741–751.

Rosenberg, H., R. G. Gerdes, and F. M. Harold. 1979. Energy coupling to the transport of inorganic phosphate in *Escherichia coli* k12. Biochemical Journal 178:133–137.

Russell, J. B., and G. M. Cook. 1995. Energetics of bacterial-growth – balance of anabolic and catabolic reactions. Microbiological Reviews 59:48–62.

Scott, J. T., J. B. Cotner, and T. M. Lapara. 2012. Variable stoichiometry and homeostatic regulation of bacterial biomass elemental composition. Frontiers in Microbiology. https://doi.org/10.3389/fmicb.2012.00042

Sterner, R. W., and J. J. Elser. 2002. Ecological stoichiometry: the biology of elements from molecules to the biosphere. Princeton University Press, Princeton, New Jersey, USA.

Tanner, R. 2002. Cultivation of bacteria and fungi. Pages 62–70 *in* C. Hurst, G. Knudsen, M. McInerney, L. Stetzenbach, and

M. Walter, editors. Manual of environmental microbiology. Second edition. ASM Press, Washington, D.C., USA.

Tempest, D. W., and O. M. Neijssel. 1978. Eco-physiological aspects of microbial growth in aerobic nutrient-limited environments. Pages 105–153 *in* M. Alexander, editor. Advances in microbial ecology. Springer US, New York, New York, USA.

Thingstad, T. F. 1987. Utilization of N, P, and organic C by heterotrophic bacteria. I. Outline of a chemostat theory with a consistent concept of 'maintenance' metabolism. Marine Ecology Progress Series 35:99–109.

Thingstad, T. F., L. Øvreas, J. K. Egge, T. Løvdal, and M. Heldal. 2005. Use of non-limiting substrates to increase size; a generic strategy to simultaneously optimize uptake and minimize predation in pelagic osmotrophs? Ecology Letters 8:675–682.

Vadia, S., and P. A. Levin. 2015. Growth rate and cell size: a re-examination of the growth law. Current Opinion in Microbiology 24:96–103.

Velji, M. I., and L. J. Albright. 1993. Improved sample preparation for enumeration of aggregated aquatic substrate bacteria. Pages 139–142 *in* P. F. Kemp, B. F. Sherr, E. B. Sherr, and J. J. Cole, editors. Handbook of methods in aquatic microbial ecology. Lewis Publishers, Boca Raton, Florida, USA.

Vrede, K., M. Heldal, S. Norland, and G. Bratbak. 2002. Elemental composition (C, N, P) and cell volume of exponentially growing and nutrient-limited bacterioplankton. Applied and Environmental Microbiology 68:2965–2971.

Zimmerman, A. E., S. D. Allison, and A. C. Martiny. 2014. Phylogenetic constraints on elemental stoichiometry and resource allocation in heterotrophic marine bacteria. Environmental Microbiology 16:1398–1410.

Supporting Information

Additional supporting information may be found in the online version of this article at http://onlinelibrary.wiley.com/doi/10.1002/ecy.1705/suppinfo